

1 Gas migration in pre-compacted bentonite under elevated pore-water pressure conditions

2 Caroline. C. Graham<sup>a\*</sup>, Jon F. Harrington<sup>a</sup> & Patrik Sellin<sup>b</sup>

3 <sup>a</sup>British Geological Survey, Keyworth, Nottingham NG12 5GG, UK

4 <sup>b</sup>Svensk Kärnbränslehantering AB, Stockholm, Sweden

5 \*Corresponding author (e-mail: caro5@bgs.ac.uk)

6 Abstract

7 Pre-compacted bentonite has long been proposed as a primary component of an  
8 engineered barrier system for the safe geological disposal of radioactive waste. Selection of  
9 properties such as the clay composition, compaction-state and clay-to-sand ratio vary in  
10 different disposal concepts. However, a sound understanding of the gas transport  
11 properties of the barrier material is often considered a necessary part of safety case  
12 development for a geological disposal facility. In this study, results are presented from two  
13 gas injection experiments conducted in Mx80 bentonite, under elevated pore-water  
14 pressure conditions. Test observations indicate that the conditions necessary for gas to  
15 enter this material are remarkably consistent, irrespective of the applied water pressure. As  
16 expected, an association is noted between the total stress experienced by the clay and the  
17 gas pressure at the moment of entry. Gas migration is interpreted as occurring by the  
18 formation and propagation of dilatant pathways within the bentonite. Local pore-pressure  
19 and stress measurements indicate that significant reworking of the clay can occur, resulting  
20 in meta-stable episodes of 'pressure-cycling', as gas seeks a stable escape pathway. These  
21 findings demonstrate the potential for 'phases' of pathway development and propagation

22 within the buffer, resulting in successive migration episodes over the repository lifetime.  
23 Experiments also show the potential for gas entry into the buffer to occur as a result of  
24 declining pore-water pressure conditions. As such, the influence of significant deviations  
25 from hydrostatic conditions (for example, resulting from glacial loading) should not be  
26 neglected when considering gas interaction with the buffer over long timescales.

27 Keywords: Bentonite; gas- flow; experiment; pore-water pressure; gas entry/breakthrough;  
28 compressibility

## 29 1 Introduction

30 In the geological disposal of high level radioactive waste (HLW), the possibility of gas  
31 generation (e.g., due to corrosion of container material/metallic waste) and radiolysis of  
32 water, is a common consideration during safety case development. In some cases, the  
33 potential for gas generation rates to exceed the rate of dissipation by diffusion must be  
34 considered (Horseman et al., 1999; SKB, 2006). Gas pressures may continue to elevate in  
35 such a scenario, until either (i) gas generation reduces sufficiently or (ii) a free gas phase is  
36 able to enter the surrounding engineered clay or host formation, in which case advective  
37 transport may occur (Sellin and Leupin, 2013). It is important to ensure that gas pressure  
38 build-up will not result in undesired effects, such as the transportation of radionuclides or  
39 mechanical damage to repository infrastructure (SKB, 2006). Given this context, a thorough  
40 understanding of the conditions under which advective gas transport will occur and the  
41 resulting evolution of such a phenomenon is a necessary consideration in the planning  
42 process for a Swedish radioactive waste repository.

43 The Swedish concept for geological disposal of radioactive waste involves the use of Mx80  
44 bentonite as part of an engineered barrier system (SKB, 2011). Vitrified waste material is  
45 enclosed within copper canisters, which are emplaced into a deposition hole within a  
46 crystalline host-rock. The void between the host-rock and the canister is then filled with  
47 blocks and pellets of pre-compacted bentonite, which provide a number of functions,  
48 including: (i) acting as a diffusional barrier surrounding the canister, and (ii) swelling on  
49 hydration (leading to the closure of voids and joints within the deposition hole).

50 In the Swedish radioactive waste disposal concept, the primary pathway for escaping gas  
51 will be through fractures present in the hostrock wall of a deposition hole. Characterisation  
52 of the granodiorite at the Äspö hard rock laboratory (and during site characterisation at  
53 Forsmark and Oskarshamn in Sweden) has shown a proportion of these fractures may be  
54 conductive (Nordqvist et al., 2008; Cuss et al., 2010). Such fractures will also enable  
55 hydration of the bentonite by the *in situ* groundwater.

56 Advective migration of a free gas phase through a porous media must involve one of two  
57 possible modes of transport: either (i) the gas passes through the original porosity of the  
58 clay, causing little disturbance to the surrounding matrix, or (ii) the gas generates new  
59 voidage through which it can migrate. The former is generally termed 'visco-capillary flow'.  
60 It is controlled by pore throat radii within the clay and the degree of water present within  
61 the pores, which must progressively be displaced in order for gas to enter (Marschall et al.,  
62 2005). The latter requires an opening (or pathway) to form resulting from applied gas  
63 pressure, accommodated for by localised deformation of the surrounding clay matrix  
64 (Marschall et al., 2005). This second mechanism is therefore generally termed 'pathway  
65 dilatancy'. Since this process essentially involves the separation of two parts of the clay

66 matrix under the action of an applied stress, it might also reasonably be described as a type  
67 of microfracture formation.

68 In the case of an unsaturated or partially saturated bentonite, a free gas phase is generally  
69 expected to migrate by conventional visco-capillary two-phase flow (Villar et al., 2012; Sellin  
70 and Leupin, 2013), since higher pressures are not required to mobilise the gas. In such cases,  
71 laboratory testing demonstrates that the applied pressure gradient will directly control the  
72 resulting gas flow rate (Villar et al., 2012). It has also been suggested that, for sand  
73 bentonite mixtures with a suitably high sand content, similar behaviour may also occur in  
74 reasonably well-saturated bentonite (Sellin and Leupin, 2013). However, in the case of fully  
75 saturated, pure bentonite, water is less mobile and pathway dilatancy is expected to occur  
76 instead (Sellin and Leupin, 2013). In such cases, gas migration at *in situ* conditions is not  
77 thought to occur unless the applied gas pressure,  $P_g$ , exceeds the total stress,  $\sigma$ , experienced  
78 by the clay (resulting from the sum of the applied water pressure and the swelling pressure,  
79  $\Pi$ ) (Horseman et al., 1999; Harrington and Horseman, 2003). Above this critical value, a  
80 mechanical interaction between the gas and clay will begin (Horseman et al., 1999;  
81 Harrington and Horseman, 2003; Birgesson and Karnland, 2013; Sellin and Leupin et al.,  
82 2013; Tawara et al., 2014), leading to the generation of pathways which allow gas transport.  
83 In order to assess the dominant form of advective gas flow in bentonite, it is therefore  
84 necessary to conduct laboratory experiments on the selected clay under the relevant  
85 boundary conditions for a given repository concept.

86 There is some degree of inconsistency in the use of certain terminology in relation to gas  
87 injection testing and care must be taken to be certain of the chosen terminology when  
88 making comparisons between studies. As such, the following definitions given for gas

89 entry, gas breakthrough and capillary entry pressure will be used for the remainder of this  
90 paper. Laboratory testing generally comprises of the application of a pressure gradient  
91 across the sample, until advective gas outflow is observed at the downstream end of the  
92 sample, at some critical value of pressure. This critical threshold is generally known as the  
93 'gas breakthrough pressure'. A further critical threshold also exists, defined as the 'gas  
94 entry pressure', which is the value at which gas first enters (or is, at least, observed to enter)  
95 the material. However, as experimental determination of gas entry can be challenging,  
96 laboratory studies often test for the 'gas breakthrough pressure' instead. The influence of  
97 declining gas pressure on gas flow is often quantified in the laboratory in terms of the  
98 'capillary threshold pressure', which is generally considered as the minimum pressure with  
99 which gas can remain mobile within the clay.

100 Experiments conducted at the laboratory scale (Horseman et al., 1997; Harrington and  
101 Horseman, 1999; Harrington and Horseman, 2003; Birgesson and Karnland, 2013; Noseck, et  
102 al., 2013) demonstrate that for pure, saturated Mx80 bentonite under expected *in situ*  
103 conditions, the primary mode of gas transport is dilatant pathway formation. Significant  
104 findings that support this conclusion include: (i) a lack of evidence for water displacement  
105 resulting from gas entry into the clay, (ii) a strong association between the stress state of  
106 the sample and the pressure required for gas to enter the clay (iii) a strong coupling evident  
107 between  $\sigma$ ,  $\Pi$  and  $P_g$  after gas breakthrough has occurred, (iv) localised changes in  $\sigma$ ,  $\Pi$  and  
108  $p_p$ , associated with the migration of gas, (v) localised outflows during gas breakthrough,  
109 which appear non-unique, (vi) the spatial evolution of gas pathways with time, evidenced by  
110 unstable flow and, (vii) no measurable desaturation in any samples (post-gas testing),  
111 indicating that gas has not passed through the bulk of the clay.

112 A number of studies also highlight evidence for gas flow by pathway dilatancy in tests  
113 involving other argillaceous materials (Ortiz et al., 2002; Angeli, et al., 2010; Cuss et al.,  
114 2010; Skurtveit et al., 2011; Harrington et al., 2012a; 2012b), as well as other studies in  
115 bentonite (Pusch et al., 1985; Namiki et al., 2014). Wiseall et al. (2015) used a specially  
116 designed pressure vessel, with a fused silica window, to directly observe the formation of  
117 discrete gas pathways during injection of Helium into kaolinite pastes. They found that  
118 these pathways were spontaneously induced above a threshold gas pressure and were  
119 observed to propagate and dilate further as gas pressure was increased. While attempts  
120 have been made to lay out a theoretical framework for this mechanism of gas flow in  
121 bentonite (Horseman et al., 1999), the capacity to generate numerical models which fully  
122 reflect the observed behaviours currently remains elusive. To begin to address this issue,  
123 two recent numerical approaches have been proposed, one using embedded fractures as  
124 conduits for gas flow (Gerrard et al., 2014) and the other linking permeability to void ratio,  
125 providing an indirect link to volume change and the stress field (Senger et al., 2014).

126 The Constant Volume Radial Flow (CVRF) apparatus used in this study was designed to  
127 simulate the generation of gas from a canister in the Swedish KBS-3 concept, with the  
128 injection rod representing a canister and the additional filter arrays simulating sinks, such as  
129 fractures, in the deposition-hole environment. Given that the primary phase of any  
130 potential gas generation is expected to occur post-thermal loading (SKB, 2006), clay samples  
131 are fully saturated before gas injection testing, as is anticipated in the Swedish concept.  
132 Results from previous CVRF experiments provide the basis for a well-developed conceptual  
133 model for gas flow in bentonite. Key features of this conceptual model are described in the  
134 following section, and are also covered by Harrington and Horseman (2003) and Graham et

135 al. (2012). In accordance with expected conditions during the most relevant scenario for gas  
136 pressure build-up in the current Swedish disposal concept, this behavioural description  
137 relates specifically to pure, fully saturated Mx80 bentonite (SKB, 2006).

## 138 **1.1 GAS MIGRATION IN BENTONITE UNDER EXPECTED HYDROLOGICAL CONDITIONS**

139 For a high-swelling clay such as bentonite, the effective stress,  $\sigma_{\text{eff}}$ , can be directly equated  
140 with the swelling pressure,  $\Pi$  (Horseman et al., 1996). In a clay–water system with the pore-  
141 water in thermodynamic equilibrium with an external reservoir of water at pressure,  $p_w$ , the  
142 total stress,  $\sigma$ , acting on a constant volume pressure vessel can therefore be expressed in  
143 terms of the effective stress law such that:

$$144 \quad \sigma = \Pi + p_w \quad (1)$$

145 This is the definition for total stress and swelling pressure used in this study and throughout  
146 the remainder of this paper.

### 147 **1.1.1 Gas entry ( $p_g > \sigma$ )**

148 In this paper we describe the gas entry phase as the point at which gas is first observed to  
149 become mobile within the clay. During laboratory testing, the exact moment of gas entry  
150 can be difficult to detect. However, a number of observations may provide evidence that  
151 entry has taken place. In particular, a notable deviation in increasing gas pressure from  
152 expected ideal gas behaviour must occur, once gas is present in the clay. Evidence from  
153 testing conducted by Harrington and Horseman (2003), and published in Graham et al.  
154 (2012) clearly demonstrates that during gas injection testing under a constant backpressure  
155 condition, gas entry is only detected after the applied gas pressure,  $p_g$ , exceeds the total  
156 stress,  $\sigma$ , experienced by the bentonite (Figure 1). In reality, this relates specifically to the

157 local stress experienced by the clay at the point of gas entry. However, even in a relatively  
158 heavily-instrumented laboratory experiment, total stress measurements may differ  
159 somewhat from those precisely where gas entry occurs. Nevertheless, the association is  
160 strong enough that it is generally apparent, even when using an average of the total stress  
161 values measured within the clay (making this value a useful comparator). The importance of  
162 locally measured stresses is more apparent at the larger scale and the association between  
163 these and gas entry has been demonstrated at the Lasgit full scale gas injection test at Äspö,  
164 Sweden (Cuss et al. 2014).

165 At the laboratory scale, observations also indicate that even, if significant quantities of gas  
166 are passed through the clay over long periods of time (and at relatively high pressure), very  
167 little water is displaced out of the bentonite during gas flow testing (Harrington and  
168 Horseman, 2003). These findings are also consistent with the assertion that advective  
169 migration of gas occurs through localised pathways, leading to little or no desaturation and  
170 a strong association between the excess gas pressure at entry and the average total stress  
171 experienced by the bentonite, which must be exceeded in order for dilatant pathways to  
172 propagate (Pusch and Forsberg, 1983; Harrington and Horseman, 1999).

173 Where the bentonite is constrained under a constant volume boundary condition, pathway  
174 propagation should result in significant perturbation of monitored stresses and pore-water  
175 pressures (Fig. 1) and such changes have, indeed, been observed during this phase of gas  
176 migration in CRVF experiments (Harrington and Horseman, 2003; Graham et al., 2012).  
177 These perturbations display time-dependent behaviour, characteristic of pathway  
178 propagation. Monitored total stresses may also display step-like responses, as pathways  
179 grow during the approach to breakthrough (Graham et al., 2012). Localised consolidation



180 may be ongoing in the near-field of opening gas pathways, which would explain  
181 observations of small-scale hydrodynamic effects that perturb the local pressure  
182 distribution within the clay.

183 While the point of gas entry in all tests displays a predictability in relation to stresses within  
184 the clay, the pressure at which gas breakthrough may occur is highly variable in comparison.  
185 This is not unexpected, given the constant volume boundary condition and the moment of  
186 breakthrough should intuitively be related to the number/geometry (or 'availability') of sink  
187 filters and the compressibility of the clay. Such effects are exacerbated in the laboratory,  
188 which may lead to the observation of high gas pressures before breakthrough (Graham et  
189 al., 2012). However, at the field scale the greater compressibility of the clay, combined with  
190 the presence of interfaces and heterogeneities, is likely to moderate extremes in behaviour  
191 and markedly reduce the likelihood of higher gas pressures, as is observed at the Lasgit  
192 field-scale gas injection experiment (Cuss et al., 2011; Graham et al., 2012). Nevertheless,  
193 the influence of sink availability and homogeneity/compressibility of the clay on gas  
194 migration behaviour should be noted. Such factors have the potential to significantly  
195 impact the maximum gas pressure likely to be sustained by the buffer at the full canister  
196 scale.

### 197 **1.1.2 Gas breakthrough ( $p_g \geq \sigma$ )**

198 Gas breakthrough occurs once a gas conducting pathway comes into contact with a sink (at  
199 laboratory scale this is a filter, but could represent a void, opening, or fracture at field scale)  
200 and is manifested by a notable outflow of gas at the backpressure pump. Gas may be  
201 mobile within the clay, but until breakthrough is reached gas pressure may continue to rise,  
202 whilst a stable outflow path is sought. Once this occurs, gas injection pressure is seen to

203 spike (Fig. 1b), displaying the characteristic first breakthrough peak in pressure reported in  
204 earlier studies (Harrington and Horseman, 1999; Horseman et al., 1999; Horseman et al.,  
205 2004). These observations can be explained by a breakdown in the tensile strength of the  
206 bentonite, leading to the sharp pressure drop after the peak (Fig. 1).

207 After peak pressure has been reached,  $p_g$  is observed to drop close to  $\sigma$ , such that;

$$208 \quad p_g \text{ (post-breakthrough)} = \sigma \approx \Pi + p_{wi} \quad (2)$$

209 In the post-gas breakthrough phase, multiple observations demonstrate a pronounced  
210 coupling between  $p_g$ ,  $\sigma$  and internal water pressure within the clay,  $p_{wi}$  (Harrington et al.,  
211 1999; Harrington and Horseman, 2003; Cuss et al., 2011; Graham et al., 2012). Likewise,  
212 monitored outflow of gas at this stage is often localised, with a non-uniform outflow  
213 distribution along the sample length. Furthermore, the distribution of flow is often seen to  
214 change abruptly and spontaneously, as localised flow alternates from one location to  
215 another (Harrington and Horseman, 2003). These findings imply an inherent instability in  
216 the nature of these gas pathways, which results in dynamic flow behaviour as their spatial  
217 distribution evolves.

### 218 **1.1.3 Shut-in response**

219 After gas breakthrough, the shut-in response of the clay can be determined by stopping the  
220 injection pump and allowing the gas pressure and resultant outflow to decay with time. As  
221 in- and out-flow cease,  $p_g$  approaches an asymptotic value that must relate to the  
222 minimum pressure at which gas is mobile in the clay (Fig. 1c). Horseman et al. (1997) and  
223 Harrington and Horseman (2003) attributed observations during shut-in to the collapse of  
224 conducting pathways in response to declining pressure, leaving a series of discontinuous,

225 'remnant' gas-filled zones within the clay (Fig. 1c). At this stage, the capillary pressure,  $p_c$ ,  
226 can be considered as the difference between the residual gas pressure,  $p_g$ , and the  
227 externally applied water pressure,  $p_w$ :

$$228 \quad p_c = p_g - p_w \quad (3)$$

## 229 **1.2 GAS MIGRATION IN BENTONITE UNDER ELEVATED PORE-WATER PRESSURE** 230 **CONDITIONS**

231 Under normal hydrostatic conditions, a strong association is apparent between the pressure  
232 at which gas entry occurs and the sum of the  $p_w$  and  $\Pi$ . However, a number of possible  
233 mechanisms may lead to noticeable deviations from such conditions during the lifetime of a  
234 repository. For example, in more Northern regions of Europe the influence of glacial loading  
235 must be considered, as it is known to influence subsurface pore-water pressure  
236 (Wildenborg, et al. 2003). Graham et al. (2014) presented experimental data indicating that  
237 such deviations may lead to a small persistent elevation in swelling pressure, even when  
238 returned to hydrostatic conditions. The cause of this hysteric behaviour remains unclear,  
239 though two possibilities include: (i) heterogeneity in the hydration behaviour of Mx80  
240 bentonite, limiting the rate at which hydraulic equilibrium is reached (Cuss et al., 2011), and  
241 (ii) permanent alteration of the clay from a double-structured to single structured  
242 microfabric, as a fully saturated state is reached (Seiphoori et al., 2014). An improved  
243 understanding of the likely impacts of this phenomenon on gas-transport characteristics of  
244 the bentonite would therefore be beneficial in assessing gas flow behaviour during pore-  
245 pressure excursions. To examine this aspect of gas flow in bentonite, the experiments  
246 presented in this study were conducted at high pore-water pressure conditions on samples  
247 previously subjected to a series of load-unload cycles (Graham et al., 2014).

248 Most gas injection experiments reported in the literature generally involve applying an  
249 excess gas pressure to a bentonite sample and increasing the pressure gradient until gas  
250 migration by advection takes place. However, given the association between gas entry  
251 pressure and total stress (itself related to the applied water pressure), it is also conceivable  
252 that gas entry may be instigated by a local decline in pore-water pressure. The experiments  
253 presented in this study were, therefore, conducted so as to explore the potential for gas  
254 entry and breakthrough to occur as a result of declining pore pressure and any associated  
255 differences in the resulting flow behaviour.

256 Data were collected from two constant volume laboratory tests investigating this scenario,  
257 as part of the EC FP-7 project Fate of Repository GasEs (FORGE). Further description of  
258 these experiments and the wider test programme are given by Graham and Harrington  
259 (2014). In contrast to the conceptual model described in Section 1.1, gas injection was  
260 carried out at elevated pore-pressure conditions and breakthrough was instigated by  
261 dropping the applied backpressure, simulating a decline in pore pressure after prior  
262 elevation. In this paper we summarise the gas migration behaviour observed and make  
263 comparison to that previously reported at expected pore-water conditions.

## 264 2 Methodology

### 265 **2.1 EXPERIMENTAL APPARATUS**

266 In order to mimic realistic down-borehole conditions, this study was focussed on laboratory  
267 testing of bentonite under a constant volume boundary condition (as would be expected in  
268 a granodiorite deposition-hole). The experiments described here were carried out using a  
269 bespoke constant volume and radial flow (CVRF) apparatus, based on a design initially

270 produced to examine the sensitivity of gas flow in compacted bentonite to the test  
271 boundary conditions (Harrington and Horseman, 2003). The CVRF apparatus consists of: (1)  
272 a thick-walled stainless steel pressure vessel, (2) a fluid injection system, (3) three  
273 independent backpressure systems, each consisting of an array of four filters acting as fluid  
274 sinks, (4) five total stress sensors to measure radial and axial stress and (5) a logging system.  
275 The steel vessel mimics the rigid deposition-hole, while the filter arrangement provides the  
276 opportunity for fluid escape, as with natural fractures cross-cutting the deposition-hole.

277 The pressure vessel (Figure 2) comprises a stainless-steel, dual-closure, tubular vessel whose  
278 end-closures are secured by twelve, high tensile cap-screws that can also apply a small pre-  
279 stress to the specimen if required, using a gauged torque-wrench. A central injection rod  
280 allows fluid to be injected directly into the middle of the test sample. Filters are also housed  
281 in the end-closures at both the injection rod end of the vessel and the downstream end.

282 The position of the sink arrays ( $p_p[1]$ , [2] and [3]) and the stress sensors ( $\sigma_{Ax\ Injection}$ ,  $\sigma_{Ax}$   
283  $_{Backpressure}$ ,  $\sigma_{rad1}$ ,  $\sigma_{rad2}$ ,  $\sigma_{rad3}$ ) are shown in Figure 2. The radial arrays contain sintered, high  
284 density, polyethylene plugs and are each connected to a separate pressure transducer.

285 Each array can also be isolated from the backpressure system and used to provide an  
286 independent measure of the local pore fluid pressure, or can be connected to the  
287 backpressure pump in order to monitor outflow. Stress measurements are made using  
288 push-rods that are each in direct contact with a miniature load cell. The central filter is  
289 embedded at the end of a 6.4 mm diameter stainless steel tube which can be used to inject  
290 the permeant, for gas flow testing purposes. The swelling of the clay samples on hydration  
291 is sufficient to seal the injection rod, which is clearly demonstrated during testing by the

292 ability to maintain high applied gas pressures with no inflow, when gas testing is initiated  
293 (see Sections 2.1 and 2.2)

294 The pressure and flow rate of test fluid is controlled and monitored using two, high-  
295 precision syringe pumps. Volume, flow rate and pressure data are then transmitted from  
296 each pump to a bespoke National Instruments logging system. Additional test parameters  
297 are logged simultaneously by the same system and the typical acquisition rate for all data is  
298 one scan every two minutes. All stress and pore pressure sensors were calibrated against  
299 laboratory standards by applying incremental steps in pressure, from atmospheric to a pre-  
300 determined maximum value, greater than that intended during experimentation. This was  
301 followed by a descending history to quantify any hysteresis, which was negligible.

302 Before injection, gas is allowed to equilibrate with water in an upstream interface vessel,  
303 ensuring that it is saturated before injection. During gas injection testing, helium was used  
304 as the permeant, due to its non-reactivity and similar molecular size to hydrogen. Because  
305 of the need to measure very small flows, testing was carried out under room temperature  
306 conditions maintained within an environmentally-controlled room, in order to minimise  
307 thermal fluctuations ( $\pm 1$  °C). It should be noted that a greater degree of noise is generally  
308 apparent for upstream flow measurements, compared to those at the downstream end.  
309 This is to be expected and reflects the large gas volume being regulated by the upstream  
310 pump, in comparison to a water reservoir at the downstream pump. Often, the  
311 downstream pump exhibits a higher degree of noise once gas breakthrough has taken place  
312 and this is apparent in some of the findings presented later in this paper (Section 2.5).

## 313 2.2 SAMPLE PREPARATION AND PROPERTIES

314 Mx80 bentonite is a fine-grained sodium bentonite, from Wyoming (United States of  
315 America), which contains around 90% montmorillonite. Blocks of pre-compacted Mx80  
316 bentonite were manufactured by Clay Technology AB (Lund, Sweden), by rapidly compacting  
317 bentonite granules in a mould under a one dimensionally applied stress (Johannesson et al.,  
318 1995). Two cylindrical specimens with a diameter of 60 ( $\pm 0.5$ ) mm and length of 120 ( $\pm$   
319 0.5) mm were sub-sampled from the pre-compacted blocks. The samples were turned on a  
320 lathe, in order to provide consistent dimensions along their entire length. A 6.35 ( $\pm 0.5$ ) mm  
321 diameter hole was then drilled into the centre of the material to accommodate the  
322 stainless-steel injection rod. The injection filter imbedded in the rod tip was machined to  
323 match the drill bit used, in shape and dimension, so as to achieve a tight fit. Care was taken  
324 to calculate the loss in clay volume as a result. Standard geotechnical properties for both  
325 samples were then calculated (pre- and post-test) and are shown in Table 1, alongside  
326 values from previous test programmes. The water content of the specimens was  
327 determined by weighing pre-test, then oven-drying (to greater than 105 °C for more than  
328 twenty-four hours) post-testing and weighing a second time. The void ratio, porosity and  
329 degree of saturation are based on an average grain density for the bentonite of 2.77 Mg.m<sup>-3</sup>  
330 (an average value, as measured by Karnland et al., 2010).

331 Samples Mx80-13 and Mx80-14 were tested under elevated pore-water pressure conditions,  
332 so as to compare behaviour with previous gas tests conducted under expected hydrostatic  
333 conditions (Harrington and Horseman, 2003; Graham et al., 2012). Geotechnical properties  
334 for these previous tests (Mx80-8 and Mx80-10) are given in Table 1, for easy comparison  
335 with the samples used in this study.

### 336 **2.3 PORE PRESSURE CYCLING**

337 Bentonite samples Mx80-10, Mx80-13 and Mx80-14 were first subjected to a pore-pressure  
338 cycling phase, in advance of gas injection testing. Hydration behaviour, swelling response  
339 and additional findings from these tests are presented by Graham et al. (2014). For  
340 reference, this part of the test history is briefly given in Table 2. This paper is focussed on  
341 the subsequent gas testing phase for samples Mx80-13 and Mx80-14.

### 342 **2.4 MX80-13**

343 Sample Mx80-13 was of notably higher density than the other bentonite samples (Table 1),  
344 most likely as a result of its slightly lower saturation state on receipt, pre-sample  
345 preparation. This initial state is consistent with a significantly higher than normal  
346 cumulative inflow observed during initial hydration of the sample (~9.5ml) and led to the  
347 generation of much larger total stresses during sample swelling as a result (Graham et al.,  
348 2014). Before gas testing, Mx80-13 was subject to incremental pore-pressure loading up to  
349 42MPa, then unloaded to 1MPa (Table 2).

350 The sample was then reloaded and allowed to equilibrate at an elevated applied water  
351 pressure of 42MPa. Monitored data for the subsequent gas testing stage are shown in  
352 Figure 3. All filters were isolated from the backpressure pump, except the central filter  
353 array ( $p_p$  [2]), allowing the local evolution of pore fluid pressure to be monitored at separate  
354 locations within the clay. Water was then swapped for helium gas as the permeant and  
355 extreme care was taken to flush any residual water from the injection rod filter, whilst at  
356 pressure. At day  $\approx$ 138 an initial gas pressure was applied to the sample through the central



357 injection rod and maintained at a constant value of 42MPa (so as to allow equilibration) for  
358 a period of approximately 11 days.

359 The injection pump was then switched to introduce gas at a constant flow rate of 40 $\mu$ l/hr  
360 (day 149), in order to generate a gradually increasing excess gas pressure with time. Over  
361 the following 18.6 day period (Figure 3a) a steady increase in locally measured pore fluid  
362 pressures was detected in the two isolated arrays ( $p_p$  [1] and  $p_p$  [3], as well as at the  
363 downstream (backpressure) end-closure. This gradual increase was also observed in the  
364 associated stresses along the length of the sample, though close inspection of the data at  
365 this time indicated that changes in pore pressure were the driving force.

366 In order to establish the nature of this flow, the injection pump was returned to constant  
367 pressure as it reached a value of 52MPa. At this stage, pore-water pressure was seen to  
368 continue to increase for several days after gas pressure was held constant. A gradual  
369 decline in pore-pressure was then observed over a period of more than 60 days, at a rate  
370 approximately three times faster than a much smaller associated decline in monitored total  
371 stresses. Since such behaviour is not expected for gas flow, this instead implies a hydro-  
372 dynamic cause and is consistent with the slow progression of a small amount of water being  
373 forced from the injection filter and into the body of the clay (despite careful flushing).  
374 These observations highlight the importance of hydrodynamic effects when monitoring such  
375 small changes in flow. In this case, the effect seems likely to be the result of 'slug flow',  
376 where small amounts of residual water remaining in the injection filter are displaced into  
377 the clay as gas pressure increases. Such behaviour would explain the observation of  
378 declining pore pressures, whilst a constant gas pressure is maintained.

379 After slug flow had ceased, the pump was returned to a constant flow of 40 $\mu$ l/hr (day 247)  
380 and excess gas pressure began to increase until it had just superseded the monitored  
381 average total stress (at around day 270). At this stage gas pressure was close to the  
382 maximum specifications for the CVRF apparatus and the rate of increase in  $p_g$  could no  
383 longer be maintained (Figure 3a). The injection pump was then reduced (at day 291.8) to a  
384 constant gas pressure of 64MPa (Fig. 3b). The outflow response observed during this initial  
385 gas stage was seen to be very small (40  $\mu$ l in around 155 days) and indicates that, even at  
386 these high pressures, gas did not enter the clay up to the value of the total stress.

387 In order to induce gas flow, the applied water pressure (shown here at the central array,  $p_p$   
388 [2]) was dropped from 42MPa to 37MPa at this stage (day 293.2) (Fig. 3b). The resulting  
389 pore pressure decline in the rest of clay was seen to be exceptionally slow and the filters in  
390 array 1 ( $p_p$  [1]) and both end-closure filters were opened to the backpressure pump at day  
391 325, to speed the equilibration process ( $p_p$  [3] was kept isolated so as to continue  
392 monitoring pore pressure evolution within the clay). This resulted in a small outflow in the  
393 downstream pump as the system re-equilibrated, followed by a gradual decline in  
394 monitored pore pressure within array  $p_p$  [3]. In spite of this, twenty days after the applied  
395 water pressure was dropped, no notable outflow had been observed, although monitored  
396 total stress did decay somewhat in response to the reduction in applied water pressure (Fig.  
397 3d). As such, the applied backpressure was dropped a further 5MPa at day 325.3 (Fig. 3c).  
398 The result was an almost immediate gas breakthrough (monitored pore-water pressure,  $p_p$   
399 [3], had only fallen by  $\sim$ 0.4MPa), indicating that the clay had already been very close to gas  
400 entry under these conditions.

401 In response to the constant gas pressure condition, gas flow was rapid after breakthrough  
402 with 25.3 litres of gas (at standard pressure and temperature) being injected into the clay  
403 over 15.7 hours. As a result, the injection pump ran out of fluid at day 325.9, causing inflow  
404 to cease and leading to a drop in the applied excess gas pressure. However, significant  
405 outflow continued until around day 330 (Fig. 3c). This behaviour would not be expected for  
406 standard visco-capillary flow, but is instead consistent with the closure of gas-filled  
407 pathways as internal  $p_g$  declines. Gas pressure was 64MPa (~8.5 MPa above the average  
408 total stress) at the point of breakthrough, but by the time outflow had ceased, the final gas  
409 pressure at the end of the test stage had declined to around 58 MPa (<2MPa above the  
410 average total stress) (Fig. 3d). Given an applied water pressure of 32MPa, this equates to an  
411 apparent capillary threshold pressure of ~26MPa.

412 Whilst the sink geometry at breakthrough makes the path taken by outflowing gas unclear,  
413 a number of observations suggest that the primary mechanism for gas migration during this  
414 test was by pathway dilation. In particular, the estimated post-test saturation of the sample  
415 Mx80-13 (Table 1) shows that the bentonite experienced very little desaturation during gas  
416 flow, in spite of more than 25 litres passing through the clay during breakthrough. Given an  
417 estimated pore volume for sample Mx80-13 of 128  $\mu\text{l}$  (>0.5% of the total outflow volume  
418 detected at the downstream filter), it is exceptionally difficult to explain the saturated  
419 sample state, post-testing, using standard concepts of visco-capillary flow (which require a  
420 significant desaturation of the clay in order for gas to migrate). These findings instead  
421 indicate that highly localised gas flow must have occurred, thereby limiting the volume of  
422 clay exposed to gas during transport through the sample. This finding and the observation  
423 that gas entry occurred relatively close to the value of the average total stress and decayed

424 close to this value during shut-in, directly contradicts behaviours expected for visco-capillary  
425 flow, where hydromechanical coupling (excluding poroelasticity) is not involved. Instead,  
426 such behaviour is highly consistent with gas flow along localised, propagating pathways,  
427 which will interact with the local stress field. Given that the former mechanism is associated  
428 with gas flow through less than fully saturated bentonite or clay/sand mixtures, whilst the  
429 latter is associated with pure, fully saturated bentonite (see Section 1), this finding is  
430 entirely as might be expected. It is, therefore concluded that pathway dilation was the  
431 primary mode of gas migration in this experiment.

## 432 **2.5 MX80-14**

433 As with sample Mx80-13, the gas injection phase of testing for Mx80-14 was carried out  
434 following hydration and a programme of pore-pressure cycling (Table 2; Graham et al.,  
435 2014). After two load-unload pore-pressure cycles, the applied water pressure was taken  
436 once more to an elevated value (41MPa) and allowed to equilibrate. Monitored data for the  
437 gas testing stage of the experiment are shown in Figure 4. An excess helium gas pressure of  
438 1MPa (42MPa in total) was then applied through the injection rod, directly into the middle  
439 of the bentonite sample (Fig. 4a, stage (1)). So as to provide observations of the pore  
440 pressure evolution during this period, all filters were isolated from the backpressure pump  
441 except those within the central filter array (monitored by  $p_p$  [2] and plotted as applied water  
442 pressure), which were used to maintain the applied water pressure boundary condition. At  
443 this stage the applied gas pressure was 5MPa below the average total stress measured  
444 within the sample. These conditions were maintained for a period of more than 50 days,  
445 during which time the monitored outflow response was negligible. No other detectable

446 signs of gas entry were observed over this period of testing, in spite of the high gas pressure  
447 condition.

448 In order to determine the impact of pore pressure decay, the applied backpressure was next  
449 reduced to 32MPa at day 225 (Figure 4a, stage (2)). Independent pore-pressure  
450 measurements were seen to decay as a result, as were the monitored total stresses within  
451 the clay. There was no evidence of gas entry into the clay during this time, including no  
452 significant outflow being detected. At day 244.4, the average total stress fell below the  
453 value of the applied gas pressure. However, clear evidence of gas entry was not apparent  
454 until  $p_g$  had fallen to the value of the highest monitored total stress (at the backpressure  
455 end-closure), which occurred on day 253. Two days subsequent to this, the presence of gas  
456 within the bentonite was indicated by a sudden increase in locally measured pore pressure  
457 at the injection end-closure filter (Fig. 4a). The measured pressure rose to a value close to  
458 the applied gas pressure at this time, and was approximately equal in magnitude to the  
459 average total stress in the clay (Figure 4a and b). Local hydrodynamic responses were also  
460 observed in the pore pressures monitored at all other local filters at this time. The pressure-  
461 pulse at the injection filter was then seen to decay over the subsequent day, demonstrating  
462 the capacity for self-sealing within bentonite.

463 This initial pressure-pulse was then followed by a series of further pulses of decreasing  
464 maximum amplitude (Fig. 4b). An associated, but less pronounced, response was also  
465 observed in the monitored total stresses within the clay, indicating that these fluctuations  
466 were pressure driven. These signals were most prominent for the sensors closest to the  
467 injection end-closure filter ( $\sigma_{Ax}$  injection and also  $\sigma_{rad1}$ ), where full gas pressure had  
468 previously been observed. At the same time, very small inflows were seen to correlate with

469 the onset of the pressure pulses (Figure 4b), though no comparable outflows were detected.  
470 This phase of 'quasi-stable' pressure cycling continued for over 30 days and is interpreted as  
471 a series of pathway opening events, which were unsuccessful in reaching a sink (Fig. 4c,  
472 stage (2)). Such prominent perturbation of the stress field during gas flow is entirely  
473 inconsistent with visco-capillary flow, but is well explained by the formation of dilatant  
474 pathways (Section 1). The frequency of these oscillations remained unstable, whilst the  
475 peak amplitude was seen to reduce with each successive event, until a phase of negligible  
476 observable activity was reached.

477 As such, a series of decreasing steps in applied water pressure (each a 5MPa reduction)  
478 were instigated (Fig. 4c, stages (3) to (5)) in order to encourage gas breakthrough. Each step  
479 was held constant until the monitored local pore pressures had fully equilibrated (a  
480 minimum of 3 weeks in each case), with the final step being to an applied water pressure of  
481 17MPa. However, the system displayed remarkable quiescence during this test stage,  
482 highlighting the ability of bentonite to sustain significant pressure gradients (25MPa for  
483 stage (5)) for substantial periods of time without major outflows and breakthrough  
484 occurring. This observation is consistent with other recent findings demonstrating the  
485 potential to sustain large pressure differentials in a range of clay-rich porous materials (Cuss  
486 et al., 2012; Cuss et al., 2014). At approximately day 392 (stage (5)), after 15 days with no  
487 change in boundary condition and apparent system quiescence, the monitored pore  
488 pressure at the injection end-closure was seen to increase sharply to the value of the  
489 applied gas pressure. At the same time, a small inflow was noted at the upstream pump.  
490 The inherent time-dependency of this behaviour can be explained by the development of a  
491 gas-filled pathway/s within the sample. Unlike the previous event, this pressure elevation

492 remained close to  $p_g$ , indicating the presence of an open and quasi-stable gas pathway,  
493 close to the injection end-closure filter. However, no notable change in outflow was  
494 observed to correlate with this event, suggesting that any gas-filled pathways had yet to  
495 intersect a filter in communication with the downstream pump (Figure 4d).

496 After a further period of negligible system activity, a significant outflow was detected at the  
497 central array on day 413.8 (Figure 4d). Local pore-pressure in the other two isolated filter  
498 arrays ( $p_p$  [1] and  $p_p$  [3]) was seen to elevate to applied gas pressure at this time, indicating  
499 the development of a gas flow pathway along the length of the sample. This highlights the  
500 potential for the clay to sustain high pressure gradients, as it implies that the majority of the  
501 pressure drop along this transmissive pathway must occur close to the point where drainage  
502 takes place. The detected outflow from the mid-array was observed to reduce dramatically  
503 soon after and this behaviour also correlated with an associated decay in pore-pressure at  
504 the neighbouring sink arrays, which was particularly pronounced for sink array  $p_p$  [1]. These  
505 observations are consistent with the opening and fragmentation/closure of localised gas-  
506 filled pathways within the clay and highlight the rapid self-sealing response of bentonite  
507 under these conditions.

508 This event was followed by a series of highly repeatable pressure pulses, measured in filter  
509 array  $p_p$  [3], as well as associated outflows (Figure 5a). Over time, the period between  
510 pressure pulses was observed to increase and outflow reduced (Fig. 5a). The clear  
511 repeatability in the onset pressure of each pulse demonstrates a pressure dependency to  
512 this phenomenon and suggests an ongoing working of the clay, resulting in a reduction in  
513 compressibility with time. Such behaviour appears to be the result of ongoing gas-driven  
514 deformation of the clay, as an exit from the system is sought. Figure 5b shows the

515 associated changes in locally measured stresses during this episodic behaviour and indicates  
516 that whilst, soon after gas entry, stresses were strongly coupled with the local pore-pressure  
517 within the clay, by day 410 only very small perturbations were observed in relation to  
518 comparatively large changes in the local pore pressures. As with observations at the field-  
519 scale (Cuss et al., 2014), this decreased sensitivity of measured stresses to pressure  
520 development suggests a transition to a regime controlled by the local gas pressure and is  
521 highly indicative of a network of transient fractures, allowing accommodation of pressure  
522 variations. At approximately day 465, pressure in the filter array  $p_p$  [3] returned to the gas  
523 injection pressure and remained at this value, indicating a stable pathway from the injection  
524 point to a filter in this array had formed.

525 Approximately 10 days later, two successive, quasi-stable periods of outflow were observed,  
526 indicating that the ability of the clay to maintain open pathways was developing further.  
527 Smaller fluctuations in the monitored pore pressure in filter array  $p_p$  [1], in association with  
528 these events, suggest a gas path to the neighbouring sink array  $p_p$  [2] had formed, most  
529 likely by way of array  $p_p$  [3]. However, the clay was still observed to self-seal effectively not  
530 long afterwards and steady-state flow was never achieved, despite the sample being  
531 subjected to significantly high gas pressures for more than 300 days. From the first  
532 observations of gas entry, perturbations within the clay were seen to be highly localised and  
533 seem to indicate changes in the gas distribution within the clay, as pathways formed and  
534 closed. This and other observations relating to gas migration processes within this test are  
535 not well explained by standard visco-capillary flow concepts, in particular the evolving  
536 periodicity noted during episodes of pressure cycling within the clay. However, findings are  
537 highly consistent with behaviours expected during the advective transport of gas by dilatant



538 pathway formation. The instability and episodic nature of gas migration observed in this  
539 experiment is discussed further in the following section.

## 540 3 Discussion

### 541 3.1.1 Pre-gas entry ( $\sigma > P_g$ )

542 Testing was carried out at elevated water pressure for samples Mx80-13 and Mx80-14,  
543 resulting in high total stresses before the injection of gas began. During the pre-gas entry  
544 phase no notable outflows were detected that could be attributed to displacement of pore  
545 water by visco-capillary action, in either test. Observations from these experiments also  
546 highlight the exceptionally high pressure gradients that Mx80 bentonite is capable of  
547 sustaining, without hydraulic outflow or gas breakthrough occurring.

### 548 3.1.2 Gas entry ( $\sigma \leq P_g$ )

549 Gas entry was reached in both tests by applying a constant gas pressure at the injection rod  
550 filter and reducing the applied backpressure to the sample. The resulting decline in locally  
551 measured pore pressures within the clay led to an associated reduction in total stress. In  
552 both experiments, gas entry was only observed to occur once the measured average total  
553 stress fell below the applied gas pressure. In this respect, the behaviour of saturated Mx80  
554 bentonite at elevated pore-water conditions appears to be similar to findings under  
555 hydrostatic conditions (Harrington and Horseman, 2003).

556 As in previous tests, observations after gas entry also display characteristics of a highly  
557 localised process, especially for Mx80-14. During this period of testing, typical observations  
558 include marked deviations from  $p_w$  of the monitored local pore pressures, which are  
559 interpreted as being perturbations in the vicinity of propagating pathways. As with previous

560 experiments, geotechnical measurements were made for both samples, before and after  
561 testing (Table 1). The resulting data show that, in spite of the high applied gas pressures  
562 and extensive periods of gas flow during later stages of gas testing (see Section 2.4), no  
563 significant desaturation of the samples occurred. Such behaviour is in-line with  
564 observations that relatively little free water is likely to be present in bentonite under these  
565 conditions (Bucher and Müller-Vonmoos, 1989). These observations are also consistent  
566 with localised, as opposed to distributed, flow through the bulk of the clay and provide  
567 further explanation for the lack of significant water outflow before gas is seen to enter the  
568 clay. The lack of desaturation and localised changes in pore fluid pressures and stresses  
569 within the sample are inconsistent with expectations for visco-capillary flow, but are well-  
570 explained by gas migration via the formation of dilatant pathways.

### 571 **3.1.3 Gas breakthrough ( $\sigma \leq P_g$ )**

572 During the gas breakthrough phase, a number of important differences were observed  
573 between the two experiments. For sample Mx80-13, breakthrough occurred soon after a  
574 step down in the applied backpressure and directly resulted in a continuous outflow from  
575 the clay. Unlike more conventional tests, the characteristic peak in total stress and local  
576 pore pressure was absent, though a marked peak in flow rate did take place at this time.  
577 The form of this response appears to be characteristic for gas breakthrough instigated by  
578 declining pore-water pressure, under a constant  $p_g$  condition (Fig. 6). In the case of Mx80-  
579 13, breakthrough occurred seemingly spontaneously, after a significant period with  
580 boundary conditions held constant. The resulting breakthrough led to a small, transient  
581 outflow, followed by relatively rapid self-sealing (on the order of days). The differences  
582 between these tests could be the result of (i) the notable discrepancy in dry density

583 between the two samples (which would influence system compressibility), (ii) small  
584 differences in sample responses during the pore-pressure cycling phase (Graham et al.,  
585 2014), (iii) the selected geometry of the hydration and outflow sinks, (iv) pre-existing  
586 weaknesses or heterogeneities within the clay, or (v) a combination of several of these  
587 factors. However, an alternative explanation is that these differences simply reflect the  
588 innate variability in the gas breakthrough process. Whilst findings from all CVRF tests to  
589 date suggest that gas entry is a highly predictable process (see Section 3.1.4), repeatability  
590 of gas breakthrough pressures has yet to be demonstrated. Nevertheless, it seems  
591 intuitively likely that less working of the clay would occur, in advance of gas breakthrough,  
592 for the higher density (and less compressible) sample, Mx80-13.

593 Although clear differences were seen between these two experiments, very high differential  
594 pressures were required in order to instigate breakthrough in both tests. This is intuitively  
595 likely, in part, to be the result of the selected sink geometry (and the associated distance to  
596 the nearest sink), but could also be a consequence of breakthrough having been instigated  
597 by a reduction in a previously elevated applied water pressure. Nevertheless, when gas  
598 pressure was allowed to decay after breakthrough of sample Mx80-13, it was observed to  
599 asymptotically approach a value close to the average total stress. This behaviour is  
600 consistent with the conceptual model for gas flow at expected hydrostatic conditions  
601 (Section 1.1.3) and implies that gas breakthrough at elevated pressures is similarly closely  
602 linked with the stress state of the sample.

603 Steady-state flow proved considerably more difficult to achieve for sample Mx80-14. Here  
604 gas flow was observed to be highly episodic and unstable in nature, alternating from one  
605 state to another in an apparently spontaneous fashion. A high propensity to self-seal was

606 also evident in the post-entry behaviour of the clay. This phase of episodic events displayed  
607 a strong cyclicity, with the pressure-controlled behaviour of the system being highly  
608 apparent (Fig. 5). Despite this seemingly repetitive behaviour, an overlying temporal  
609 evolution in response was also observed, which displayed characteristics consistent with a  
610 continued working of the clay, until a more stable outflow could finally take place.

611 However, since this behaviour was not observed in both tests it seems likely that the  
612 elevated pore-water pressure condition is not the primary cause of this behaviour. A more  
613 plausible control is the influence of sink filter geometry in these tests, as in both cases only  
614 one filter array was made available as a sink for gas escape, reducing the likelihood of a gas  
615 pathway intersecting a sink and resulting in an inherently unstable system. Similar  
616 observations have been made at the Lasgit field test, where gas was detected migrating  
617 around the canister interface before it could eventually escape (Cuss et al., 2014). The  
618 reduced compressibility of sample Mx80-13 might also explain the lack of a similar  
619 reworking occurring before major breakthrough, resulting from the notably higher initial  
620 density in this test.

621 The cyclic behaviour observed in test Mx80-14 would, therefore, represent an 'end-  
622 member' phenomenon; the consequence of a semi-compressible system where gas escape  
623 has not yet become possible. If correct, this implies that such behaviour may well also occur  
624 on long timescales in a repository, for example in a situation where flow pathways are so  
625 long that they are inherently unstable and unable to maintain a continuous pathway for  
626 drainage of gas. Nevertheless, the controls influencing the duration and likelihood of this  
627 form of behaviour and the approach to steady-state flow, require further investigation.

#### 628 **3.1.4 Implications**

629 Dilatancy has been included in some recent numerical models, in order to represent the  
630 processes involved more accurately (Gerard et al., 2014; Senger et al., 2014, Tawara et al.,  
631 2014). However, there is currently a paucity of data relating to the spatial distribution and  
632 temporal evolution of gas pathways involved in this process (SKB, 2006), which is limiting  
633 further numerical model development at present (Harrington et al., 2012). Given the  
634 requirement to image gas pathways within a representative volume whilst under pressure,  
635 progress is challenging. An alternative approach is to utilise the observed threshold  
636 dependency of gas migration during repository design, so as to mitigate against this  
637 eventuality. High precision experiments, monitoring multiple parameters independently,  
638 have been used to develop a detailed conceptual model relating gas entry to total stress  
639 within the clay (Section 1.1; Harrington and Horseman, 2003). This model exhibits a high  
640 degree of predictability and is consistent with findings in this and previous studies (Pusch et  
641 al., 1985; Pusch and Forsberg, 1983). A cross-plot showing key parameters for several Mx80  
642 bentonite gas injection tests is shown in Figure 7. Data here are compiled from this study,  
643 from previous work of Harrington and Horseman (2003) and from the full-scale gas injection  
644 test Lasgit, at the Äspö Hard Rock Laboratory in Sweden (Cuss et al., 2014). Despite the  
645 different test conditions (and dry densities) covered by the experimental data used, an  
646 association between gas entry and stress state is highly apparent.

647 A significant amount of experimentally-generated data and associated process  
648 understanding is now available to numerate this conceptual model. Such a model provides  
649 a sound foundation from which to draw on when attempting to understand and the  
650 conditions under which gas migration might occur in a repository. Evidence from laboratory

651 testing indicates that, were such migration to occur, it is unlikely to lead to the displacement  
652 of large volumes of water (which would be unfavourable should soluble radionuclide release  
653 from the wastefrom have taken place).

654 There is, however, one potential exception to this, which cannot be excluded at the present  
655 time. It is conceivable that the application of high gas pressures, over significant periods of  
656 time, could possibly lead to bulk compression and drainage of the clay (Harrington and  
657 Horseman, 2003; Sellin and Leupin, 2013). The potential for this phenomenon is currently  
658 not well understood, especially since the effect is only likely to be of significant magnitude  
659 over long timescales. However, one favourable aspect of the material performance over the  
660 long term is its propensity to 'self-seal' after a gas migration event. The laboratory  
661 experiments outlined in this paper demonstrate this capacity, with clay seemingly  
662 recovering its barrier characteristics rapidly, even between individual gas migration events.  
663 Harrington and Horseman (2003) also observed that this behaviour was further assisted by  
664 rehydration of the clay, which notably reduces prior 'memory' of gas migration and restores  
665 the clay close to its original state.

666 Findings presented here suggest that the relationship between gas entry pressure and  
667 locally measured total stresses is consistent with the conceptual model for gas entry given  
668 at lower pore-pressures (Section 1.1), irrespective of previous test history. Observations in  
669 both these experiments indicate that the subsequent advective transport of gas is also  
670 consistent with this model, and occurs via the propagation of localised, dilatant pathways.  
671 It, therefore, seems unlikely that excursions from expected hydrostatic conditions in the  
672 repository will impact on the current model for gas entry behaviour of bentonite. One  
673 consequence of this which should be noted is that during such an excursion, a bentonite

674 barrier will be capable of sustaining higher gas pressures before entry takes place. This  
675 capacity is likely to continue over the timescales necessary for the clay to return to hydraulic  
676 equilibrium. However, it is much less trivial to draw conclusions on the influence of prior  
677 pore-pressure cycling upon the behaviour of migrating gas, once it has entered the clay.  
678 The differences in the approach to gas breakthrough in these two tests make comparison  
679 particularly difficult, especially considering repeatability of behaviour at this stage of gas  
680 flow is not easy to achieve, even in tests where initial conditions and materials are  
681 comparable. However, it is conceivable that any change in compressibility of the clay  
682 resulting from loading may influence the approach from gas entry to breakthrough.

683 Observations relating to the post-gas entry phase provide insight into the evolution of the  
684 system as it approaches breakthrough. In particular, a progressive time-dependent  
685 evolution is observed during this phase, resulting from a re-working of the clay until a more  
686 stable flow regime can be established. If the clay is relatively incompressible under the  
687 applied pressure conditions, this phase may be short and less apparent before breakthrough  
688 occurs. However, if the clay is able to accommodate a degree of compression and gas is  
689 unable to find a sink, a constant pressure condition alone may be enough to energise the  
690 system sufficiently for continued evolution. This behaviour may be sustained for significant  
691 periods of time, while gas continues to seek a sink, and can result in seemingly spontaneous  
692 changes (though it is likely this is a result of limitations in the number of points of  
693 observation within the material). This alternation in system behaviour, from one meta-  
694 stable state to another, is clearly gas pressure-driven and appears to be highly unpredictable  
695 in nature. Observations suggest that any subsequent decline in ambient pore-water  
696 pressure also has the potential to further destabilise the system and lead to additional

697 episodes of pathway propagation, though this is not a necessary condition for such  
698 behaviour. It is not yet clear whether repeated breakthrough events may lead to  
699 progressive reworking of the clay over long timescales. Findings from these experiments  
700 and those of Harrington and Horseman (2003) indicate that the presence and distribution of  
701 sinks (ie. conductive fractures/faults) within the deposition-hole will, therefore, be of  
702 primary importance to the duration and nature of this phase of gas migration, both under  
703 normal and elevated  $p_w$  conditions.

#### 704 4 Conclusion

705 A primary objective of this work is to examine the influence of sustained periods of pore  
706 pressure elevation and consequent decline upon the swelling and gas flow properties of a  
707 bentonite buffer. Pore pressure cycling experiments were carried out on two Mx80  
708 bentonite samples under constant volume conditions. Both samples were subjected to gas  
709 injection at an elevated pore pressure condition, following a phase of pore-pressure cycling.  
710 The consequent observations indicate that characteristics of the gas entry process are  
711 similar to those observed in comparable experiments conducted at lower applied water  
712 pressures. As with tests conducted under more conventional boundary conditions (see  
713 Section 1.1), there is an association between gas pressure and total stress after gas  
714 breakthrough. Unlike the majority of gas injection experiments on bentonite, gas entry was  
715 instigated by maintaining a constant gas pressure and reducing the applied water pressure  
716 incrementally. The pressure at which the onset of gas entry occurred was consistent with  
717 previous observations at hydrostatic conditions and appears to be relatively predictable.  
718 As with previous studies conducted at lower pore pressures, the findings from these  
719 experiments are best explained by dilatant pathway formation as the primary mechanism



720 for gas flow through the clay. In contrast, standard concepts of visco-capillary flow cannot  
721 explain observed hydromechanical coupling or a lack of desaturation of the clay after  
722 testing.

723 Observations from both tests highlight the capacity of Mx80 bentonite to sustain very large  
724 stress gradients over significant periods of time. In one test, gas entry and breakthrough  
725 occurred close together, with very little evidence of reworking of the clay being apparent.  
726 In the other test, highly episodic and unstable gas flow was observed, displaying meta-stable  
727 qualities. This behaviour is interpreted as a consequence of gas being unable to escape,  
728 whilst the system remains energised. Such behaviour is consistent with the development of  
729 temporally evolving and potentially spatially unique gas pathways, suggesting that the time  
730 to breakthrough and the associated breakthrough pressure may not be repeatable, even for  
731 the same test methodology. Whilst, this behaviour was not observed for the other test, it is  
732 proposed that these observations result from ongoing deformation of the clay, whilst gas is  
733 unable to escape the system, rather than being a consequence of the elevated pore  
734 pressure history. This hypothesis is an intuitive one, since meta-stability is a likely feature of  
735 such conditions in bentonite, where the propagation front of a gas pathway is the most  
736 unstable part of the system (Harrington and Horseman, 2003). This would seem to indicate  
737 that the degree of compressibility of the clay may be an important control on the approach  
738 to gas breakthrough in the buffer.

739 Findings from this study highlight the remarkable consistency of gas flow behaviour for  
740 pure, saturated bentonite, with stress conditions playing a crucial role irrespective of pore-  
741 water pressure conditions. Laboratory evidence also indicates the potential for gas entry to  
742 occur as a result of declining pore-water pressure in a repository environment. Whilst the

743 controls on this behaviour appear no different from a more conventional approach to  
744 breakthrough, the form of the resulting response differs somewhat, with the characteristic  
745 break-through 'peak-pressure' no longer apparent. Perhaps more crucially, these findings  
746 demonstrate that deviations in pore water pressure (for example, resulting from glacial  
747 unloading) represent a potential mechanism for gas entry into the buffer and must  
748 therefore not be neglected when considering gas generation scenarios in a repository  
749 environment.

750

751 **Acknowledgements:**

752 The research leading to these results has received funding from Svensk  
753 Kärnbränslehantering AB and the European Atomic Energy Community's Seventh  
754 Framework Programme (FP7/2007-2011) under Grant Agreement no. 230357, the FORGE  
755 project. We would like to thank Robert Cuss for productive discussion, comments and  
756 resulting improvements. Thanks also go to the Research and Development Workshops at  
757 the British Geological Survey, for their involvement in the design and manufacture of the  
758 test apparatus. This paper is published with the permission of the Executive Director of the  
759 British Geological Survey (NERC). Thanks also to the reviewers, for their time and helpful  
760 comments.

761

762

763

764

765 **References:**

- 766 Angeli, M. Solday, M., Skurtveit, E. and Aker, E , 2009. Experimental percolation of supercritical CO2 through a  
767 caprock, *Energy Procedia*, 1, 3351-3358.
- 768 Birgersson, M. and Karnland, O., 2013. Gas Intrusion in Bentonite—Results of Small Scale Experiments. In *Gas  
769 Generation and Migration International Symposium and Workshop, 5th to 7th February 2013 Luxembourg* (p.  
770 15).
- 771 Bucher, F. and Müller-Vonmoos, M., 1989. Bentonite as a containment barrier for the disposal of highly  
772 radioactive wastes. *Applied Clay Science*, 4, 157-177.
- 773 Cuss, R.J., Harrington, J.F., and Noy, D.J., 2010. Large scale gas injection test (Lasgit) performed at the Äspö  
774 Hard Rock Laboratory. Summary report 2008. Svensk Kärnbränslehantering AB (SKB) Technical Report TR-10-  
775 38, SKB, Stockholm, Sweden.
- 776 Cuss, R. J., Harrington, J. F., Noy, D. J., Wikman, A., & Sellin, P., 2011. Large scale gas injection test (Lasgit):  
777 Results from two gas injection tests. *Physics and Chemistry of the Earth, Parts A/B/C*, 36(17), 1729-1742.-
- 778 Cuss, R.J., Harrington, J.F. Graham, C.C., Sathar, S., Milodowski, A.E., 2012. Observations of stable high-  
779 pressure differentials in clay-rich materials; implications for the concept of effective stress. *Mineral Mag*, 76 (8)  
780 (2012), pp. 3115–3129.
- 781 Cuss, R.J., Harrington, J.F., Graham, C.C. and Noy, D.J., 2014. Observations of Pore Pressure in Clay-rich  
782 Materials; Implications for the Concept of Effective Stress Applied to Unconventional Hydrocarbons. *Energy  
783 Procedia*, 59, 59-66.
- 784 Gerard, P., Harrington, J., Charlier, R. and Collin, F., 2014. Modelling of localised gas preferential pathways in  
785 claystone. *International journal of rock mechanics and mining sciences*, 67, pp.104-114.
- 786 Graham, C.C., Harrington, J.F., Cuss, R.J. and Sellin, P., 2012. Gas migration experiments in bentonite:  
787 implications for numerical modelling. *Mineralogical Magazine*, 76(8), pp.3279-3292.
- 788 Graham, C.C. and Harrington, J.F., 2014. Final Report of FORGE 3.2.1: Key gas Migration Process in Compact  
789 Bentonite, BGS Commissioned Report, FORGE FP7 D3.33, CR/14/064, 60pp.
- 790 Harrington, J.F. and Horseman, S.T., 1999. Gas transport properties of clays and mudrocks. In: *Muds and  
791 Mudstones: Physical And Fluid Flow Properties* (eds A.C.Aplin, A.J. Fleet, and J.H.S. Macquaker). Geological  
792 Society of London, Special Publication No. 158, 107–124.
- 793 Harrington, J.F. and Horseman, S.T., 2003. Gas migration in KBS-3 buffer bentonite: Sensitivity of test  
794 parameters to experimental boundary conditions. Report TR-03-02. Svensk Kärnbränslehantering AB (SKB),  
795 Stockholm, Sweden.
- 796 Harrington, J.F. and Birchall, J.D., 2007. Sensitivity of total stress to changes in externally applied water  
797 pressure in KBS-3 buffer bentonite. Svensk Kärnbränslehantering AB (SKB), Stockholm, Sweden, SKB Silver  
798 Series Technical Report TR-06-38.
- 799 Harrington, J.F., de La Vaissière, R., Noy, D.J., Cuss, R.J. and Talandier, J., 2012a. Gas flow in Callovo-Oxfordian  
800 Clay (COx): Results from laboratory and field-scale measurements. *Mineralogical Magazine*, 76, 8, 3303-3318.  
801
- 802 Harrington, J.F., Milodowski, A.E., Graham, C.C., Rushton, J.C. and Cuss, R.J., 2012b. Evidence for gas-induced  
803 pathways in clay using a nanoparticle injection technique. *Mineralogical Magazine*, Vol. 76, 8, 3327-3336.

804 Horseman, S.T., Higgo, J.J.W., Alexander, J. and Harrington, J.F., 1996. Water, gas and solute movement in  
805 argillaceous media. Prepared by British Geological Survey for NEA SEDE working group on measurement and  
806 physical understanding of groundwater flow through argillaceous media. OECD Nuclear Energy Agency, Report  
807 CC-96/1.

808 Horseman, S.T., Harrington, J.F. and Sellin P., 1997. Gas Migration In Mx80 Buffer Bentonite. In: Proc. Scientific  
809 Basis For Nuclear Waste Management XX, Boston, 2–6 Dec., 1996 (eds W.J. Gray And I.R. Triay), MRS Symposia  
810 Proceedings, 465, Materials Research Society, Warrendale, Pennsylvania, 1003–1010.

811 Horseman, S.T., Harrington, J.F., and Sellin, P., 1999. Gas migration in clay barriers, *Engineering Geology*, 54, 1-  
812 2, 139-149.

813 Horseman, S.T., Harrington, J.F. and Sellin, P., 2004. Water and gas flow in Mx80 bentonite buffer clay. In:  
814 Symposium on the Scientific Basis for Nuclear Waste Management XXVII (Kalmar), Materials Research Society,  
815 807, 715-720.

816 Johannesson, L.-E., Börgesson, L. and Sandén, T., 1995. Compaction of bentonite blocks: Development of  
817 technique for industrial production of blocks which are manageable by man. *Svensk Kärnbränslehantering AB*,  
818 TR 95-19.

819 Karnland, O., 2010. Chemical and mineralogical characterization of the bentonite buffer for the acceptance  
820 control procedure in a KBS-3 repository, Report TR-10-60. *Svensk Kärnbränslehantering AB (SKB)*, Stockholm,  
821 Sweden.

822 Marschall, P., Horseman, S. and Gimmi, T., 2005. Characterisation of gas transport properties of the Opalinus  
823 Clay, a potential host rock formation for radioactive waste disposal. *Oil & gas science and technology*, 60(1),  
824 pp.121-139.

825 Namiki, K., Asano, H., Takahashi, S., Shimura, T. and Hirota, K., 2014. Laboratory gas injection tests of  
826 compacted bentonite buffer material for TRU waste disposal. *Geological Society, London, Special Publications*,  
827 400(1), pp.521-529.

828 Noseck, U., Capouet, M., Rübél, A. and Sillen, X., 2013. FORGE: General outcomes: A view from the general  
829 rapporteurs. Birgersson, M. and Karnland, O., 2013. Gas Intrusion in Bentonite—Results of Small Scale  
830 Experiments. In *Gas Generation and Migration International Symposium and Workshop, 5th to 7th February*  
831 *2013 Luxembourg* (p. 15).

832 Nordqvist, R., Gustafsson, E., Andersson, P. and Thur, P., 2008. Groundwater flow and hydraulic gradients in  
833 fractures and fracture zones at Forsmark and Oskarshamn. *Svensk Kärnbränslehantering AB (SKB) Report*, R-  
834 08-103.

835 Ortiz, L., Volckaert, G. and Mallants, D., 2002. Gas generation and migration in Boom Clay, a potential host rock  
836 formation for nuclear waste storage, *Engineering Geology*, 64, 287-296.

837 Pusch, R. and Forsberg, T., 1983. Gas migration through bentonite clay. *SKB Technical Report 83-71*,  
838 Stockholm, Sweden.

839 Pusch, R., Ranhagen, L. and Nilsson, K., 1985. Gas migration through Mx-80 bentonite. *Nagra Technical Report*  
840 *NTB 85-36*, Wettingen, Switzerland.

841 Seiphoori, A., Ferrari, A. and Laloui, L., 2014. Water retention behaviour and microstructural evolution of MX-  
842 80 bentonite during wetting and drying cycles. *Géotechnique*, 64(9), pp.721-734.

843 Sellin, P. and Leupin, O.X., 2013. The use of clay as an engineered barrier in radioactive-waste management—a  
844 review. *Clays and Clay Minerals*, 61(6), pp.477-498.

845 Senger, R., Romero, E., Ferrari, A. and Marschall, P., 2014. Characterization of gas flow through low-  
846 permeability claystone: laboratory experiments and two-phase flow analyses. Geological Society, London,  
847 Special Publications, 400(1), pp.531-543.

848 Skurtveit, E., Aker, E., Soldal, M., Angeli, M. and Hallberg, E., 2010. Influence of micro fractures and fluid  
849 pressure on sealing efficiency of caprock: a laboratory study on shale, GHGT-10.

850 Svensk Kärnbränslehantering AB (SKB), September 2006. Buffer and backfill process report for the safety assessment SR-  
851 Can, TR-06-18.

852 Svensk Kärnbränslehantering AB (SKB), March 2011. Long-term safety for the final repository for spent nuclear fuel at  
853 Forsmark: Main report of the SR-Site project, TR-11-01.

854 Tawara, Y., Hazart, A., Mori, K., Tada, K., Shimura, T., Sato, S., Yamamoto, S., Asano, H. and Namiki, K., 2014.  
855 Extended two-phase flow model with mechanical capability to simulate gas migration in bentonite. Geological  
856 Society, London, Special Publications, 400(1), pp.545-562.

857 Villar, M.V., Martín, P.L., Romero, F.J., Barcala, J.M. and Gutiérrez-Rodrigo, V., 2012. Gas transport through  
858 bentonite: influence of dry density, water content and boundary conditions. *Propriétés de Transfert des*  
859 *Géomatériaux*. Transfert, 2012, pp.379-389.

860 Wildenborg, AFB, Orlic, B, Thimus, JF, Lange, G, De Cock, S, De Leeuw, CS, De Veling, EJ, M., 2003. Radionuclide  
861 transport in clay during climate change, *Netherlands Journal of Geosciences/Geologie En Mijnbouw* 82(1), 19–  
862 30.

863

864

865

866

867

868

869

870

871

872

873

874

875

876 **Tables:**

877 **Table 1** – Geotechnical properties of the test specimens, before and after testing.

Sample	Study	Before testing					After testing
		Water content (%)	Bulk density (Mg.m <sup>-3</sup> )	Dry density (Mg.m <sup>-3</sup> )	Void ratio	Saturation (%)	Saturation (%)
<b>Mx80-8</b>	<i>Harrington and Horseman (2003)</i>	26.7	1.997	1.577	0.756	97.6	≥100 <sup>1</sup>
<b>Mx80-10</b>	<i>Harrington and Horseman (2003); Harrington and Birchall (2007); Graham et al. (2014)</i>	26.7	2.005	1.582	0.751	98.6	≥100 <sup>1</sup>
<b>Mx80-11</b>	<i>Harrington and Birchall (2007); Graham et al. (2014)</i>	25.6	2.016	1.605	0.726	97.6	≥100 <sup>1</sup>
<b>Mx80-13<sup>2</sup></b>	<i>This study; Graham et al. (2014)</i>	20.1	2.064	1.718	0.612	91.1	≥100 <sup>1</sup>
<b>Mx80-14</b>	<i>This study; Graham et al. (2014)</i>	26.6	1.999	1.579	0.754	97.7	≥100 <sup>1</sup>

878

879

880

<sup>1</sup> Measured value indicates sample was fully saturated, within uncertainty limits of the measurement.

<sup>2</sup> Mx8-13 was sub-sampled from a pre-compacted bentonite block with a notably lower initial saturation, leading to a higher starting dry-density than the other test specimens.

881 **Table 2** – Test history for the samples subjected to pore-pressure cycling (reported by  
 882 Graham et al., 2014), before gas injection testing.

Sample	Mx80-10		Mx80-13		Mx80-14	
Stage	Applied $p_w$ (MPa)	Ave. total stress (MPa)	Applied $p_w$ (MPa)	Ave. total stress (MPa)	Applied $p_w$ (MPa)	Ave. total stress (MPa)
1	1.0	6.3	1.0	22.1	0.9	6.7
2	2.0	7.0	6.0	26.6	11.0	16.2
3	3.0	7.9	24.1	43.1	20.9	25.8
4	4.0	8.7	42.2	60.0	10.8	16.0
5	5.0	9.7	24.1	45.7	1.0	6.9
6	6.0	10.6	6.0	29.4	20.7	25.5
7	7.0	11.5	1.0	25.2	30.7	35.1
8	4.0	9.6	6.0	27.9	40.7	45.0
9	1.0	7.4	24.1	43.3	30.8	36.0
10	---	---	42.2	59.6	20.8	26.4
11	---	---	---	---	1.3	7.0

883  
 884  
 885  
 886  
 887  
 888

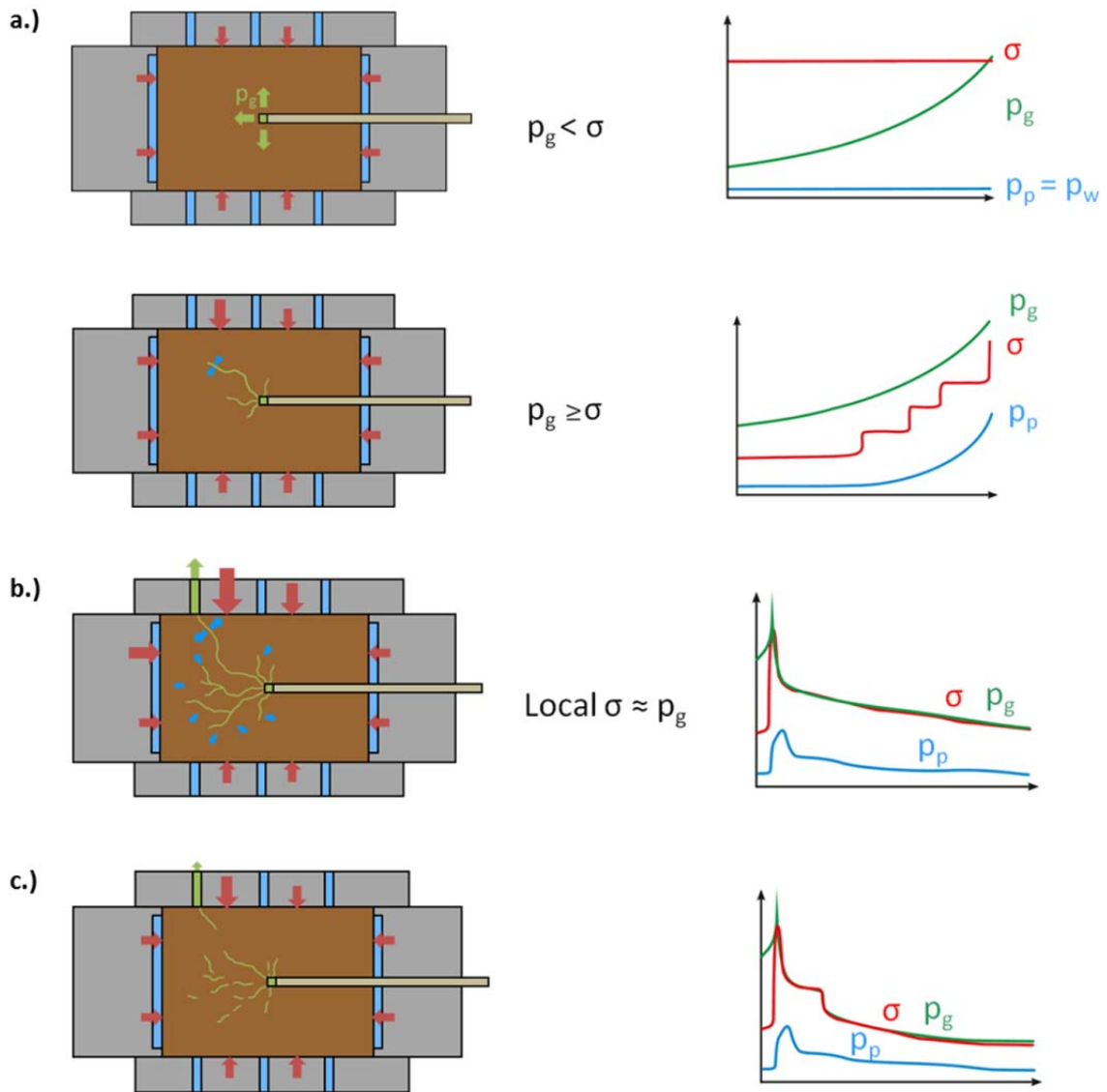
889 **Table 3** – Gas injection test history for samples Mx80-13 and Mx80-14. EQ = equilibration,  
 890 CP = Constant pressure, CF=Constant flow rate, SI = gas injection stopped and pressure  
 891 allowed to decay.

Sample	Mx80-13				Mx80-14			
Stage	Stage type	Applied $p_g$ (MPa)	Gas flow rate ( $\mu\text{l/h}$ )	Applied $p_w$ (MPa)	Stage type	Applied $p_g$ (MPa)	Gas flow rate ( $\mu\text{l/h}$ )	Applied $p_w$ (MPa)
<b>Equilibration</b>	EQ	---	---	42	EQ	---	---	41
<b>1</b>	CP	42	---	42	CP	42	---	41
<b>2</b>	CF	---	40	42	CP	42	---	32
<b>3</b>	CP	52	---	42	CP	42	---	27
<b>4</b>	CF	---	40	42	CP	42	---	22
<b>5</b>	CP	64	---	42	CP	42	---	17
<b>6</b>	CP	64	---	37	---	---	---	---
<b>7</b>	CP	64	---	32	---	---	---	---
<b>8</b>	SI	57 <sup>3</sup>	---	32	---	---	---	---

892  
 893  
 894  
 895  
 896  
 897  
 898  
 899

<sup>3</sup> At end of shut-in, once further pressure decay was negligible.





901

902 **Figure 1** – Schematic representation of gas injection in Mx80 bentonite under a constant volume  
 903 boundary condition.

904 a.) Gas entry under a constant flow rate gas injection. The internal pore-pressure,  $p_p$ , is initially  
 905 equal to applied water pressure,  $p_w$ . Entry only occurs once gas pressure exceeds the total  
 906 stress,  $\sigma$ , experienced by the bentonite. Consolidation may also occur in the near-field of  
 907 propagating pathways, leading to small-scale hydrodynamic effects in their vicinity.

908 b.) Gas breakthrough response under constant flow rate gas injection. Breakthrough occurs  
909 when a propagating gas pathway intersects a sink, allowing major outflow to occur and causing  
910 the applied gas pressure to peak. This characteristic response is followed by gas pressure falling  
911 to the value of the locally measured total stress, as gas pathways stabilise and steady-state flow  
912 is achieved.

913 c.) Shut-in response as constant gas flow is halted and pressure allowed to decline. As gas  
914 pathways collapse, outflow downstream is seen to fall, whilst declining stresses and gas pressure  
915 asymptote towards a value which is close to the sum of the swelling pressure and the applied  
916 water pressure. Residual gas is left in localised regions of the bentonite and may well impact the  
917 peak pressure required to achieve breakthrough in following gas injection episodes.

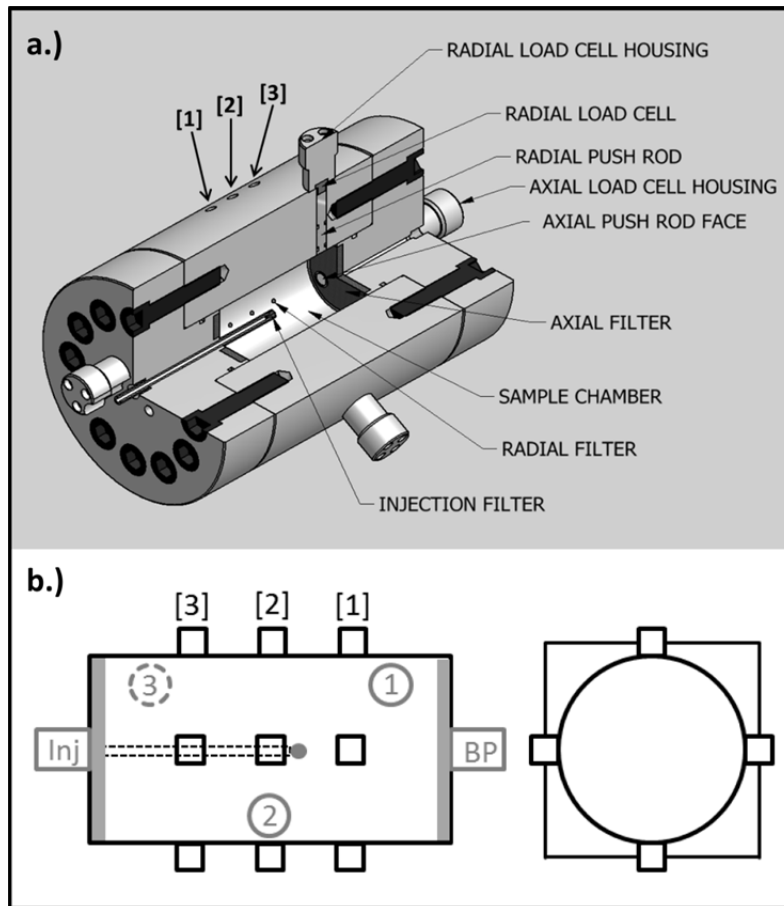
918

919

920

921

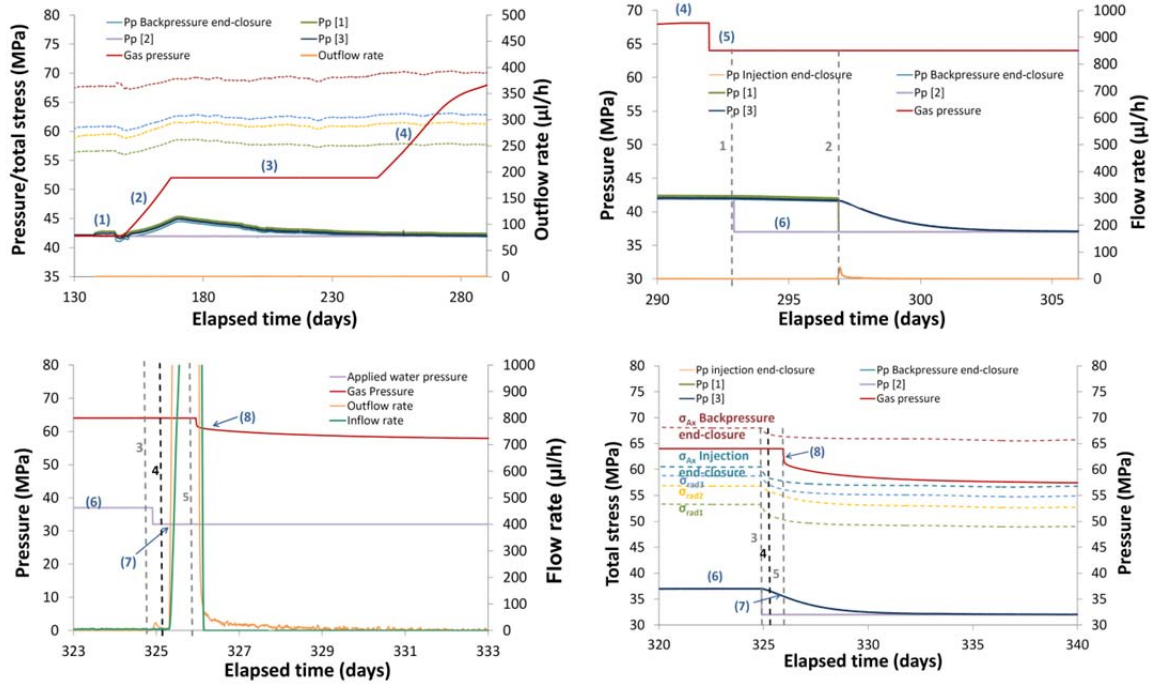
922



923

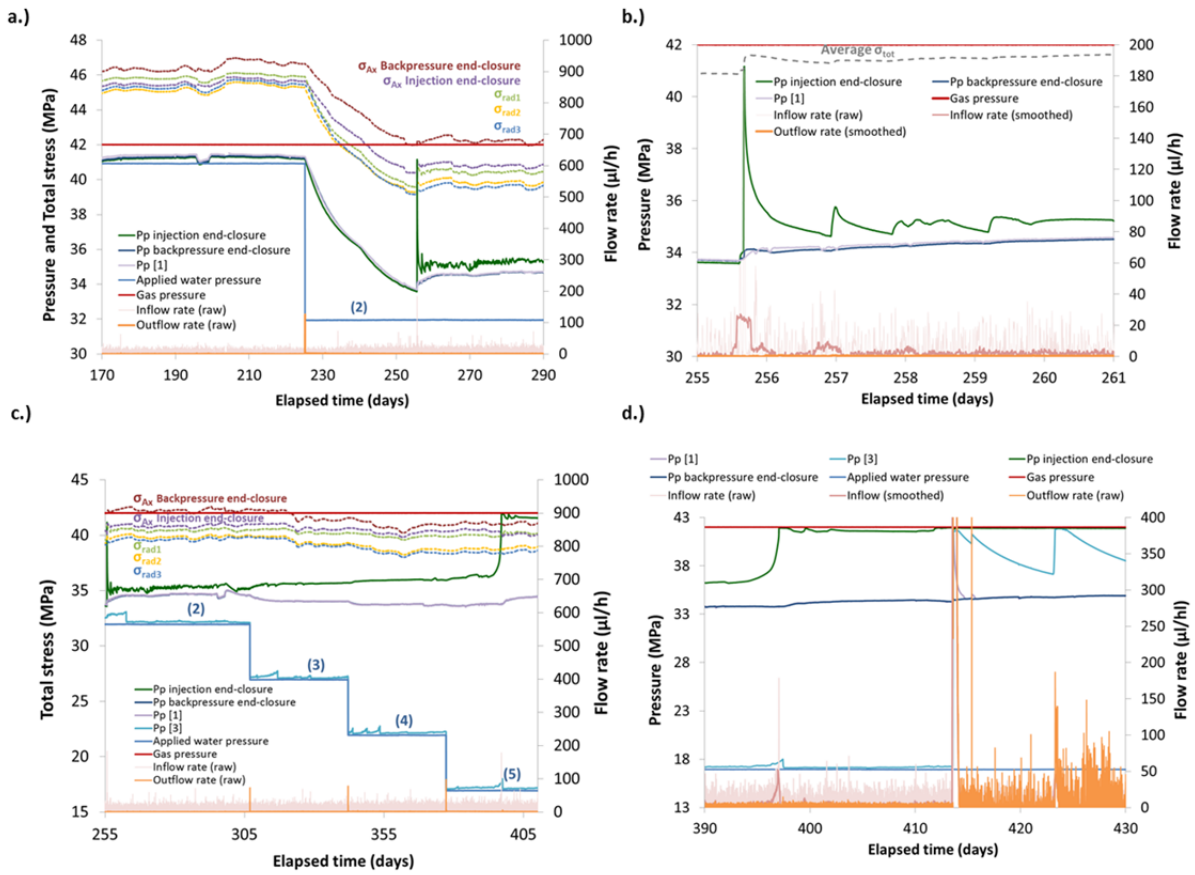
924 **Figure 2** – The Constant Volume Radial Flow (CVRF) cell in a.) cutaway, showing the two end-closures  
 925 and drainage filters, the central fluid injection filter, the input ports for the radial sink arrays and the  
 926 push rod arrangement, and b.) sensor locations: (i) axial total stress at the injection and  
 927 backpressure end-closures (grey rectangles) –  $\sigma_{Ax}$  Injection,  $\sigma_{Ax}$  Backpressure, (ii) radial total  
 928 stresses in three independent locations (grey circles) –  $\sigma_{rad1}$ ,  $\sigma_{rad2}$ ,  $\sigma_{rad3}$ , (iii) porous filters embedded  
 929 in the injection and backpressure end-closures (shaded grey rectangles) and the tip of the gas  
 930 injection rod (shaded grey circle) are connected to independent pore pressure transducers –  $p_p$   
 931 Injection,  $p_p$  Backpressure and  $p_g$  (gas) and (iv) three sink arrays (black squares), each linking four  
 932 porous filters to a pore pressure transducer –  $Pp[1], [2], [3]$ .

933



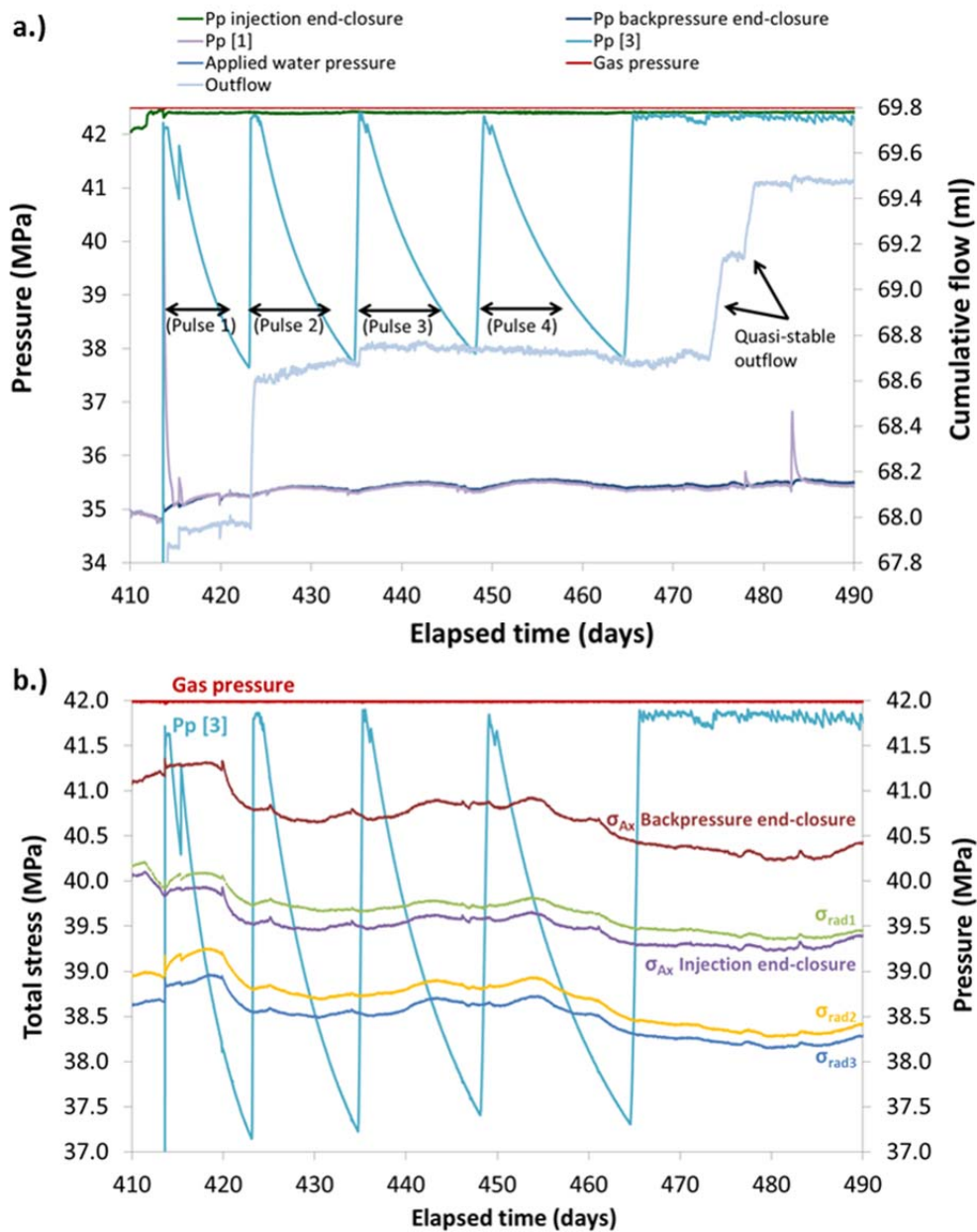
934

935 **Figure 3** – Sample Mx80-13. a.) System response to an applied gas pressure ramp. An increase in  
 936 locally measured pore pressures is attributed to the occurrence of ‘slug flow’. Pore pressures slowly  
 937 returned to the value of the applied water pressure ( $p_p$  [2]), after gas pressure was held constant. A  
 938 second pressure ramp, led to a decline in the rate of pressurisation, as gas pressure reached the  
 939 maximum specifications of the apparatus. b.) Local pore pressure decline, resulting from a reduction  
 940 in the applied water pressure ( $p_p$  [2], dashed line 1) was slow and the filters in array 1 ( $p_p$  [1]) and  
 941 both end-closure filters were opened to the backpressure pump, speeding equilibration (dashed  
 942 line 2). c.) Gas breakthrough occurred by day 325 (dashed line 4), after applied water pressure was  
 943 reduced (dashed line 3). The injection pump ran out of fluid at day 325.9 (dashed line 5) and inflow  
 944 ceased, resulting in a drop in applied gas pressure and a reduction in outflow. d.) Stress decline  
 945 following a step down in applied water pressure (dashed line 3), leading to gas breakthrough  
 946 (dashed line 4). Once gas pressure was allowed to decay (dashed line 5), it approached a value close  
 947 to the average total stress in the clay.



948

949 **Figure 4** – Sample Mx80-14. a.) Test history for the first 80 days of gas injection. Gas entry was first  
 950 detected when gas reached the injection end-closure filter (day ~ 255), b.) Gas injection history,  
 951 post-entry into the bentonite. The clay sustained significant pressure gradients (up to 25MPa for  
 952 stage (5)) with no major outflow occurring, c.) At gas entry, small inflows correlate with pressure-  
 953 pulses, d.) Pore-pressure in arrays  $p_{p1}$  and  $p_{p3}$  reach gas pressure, before decaying.

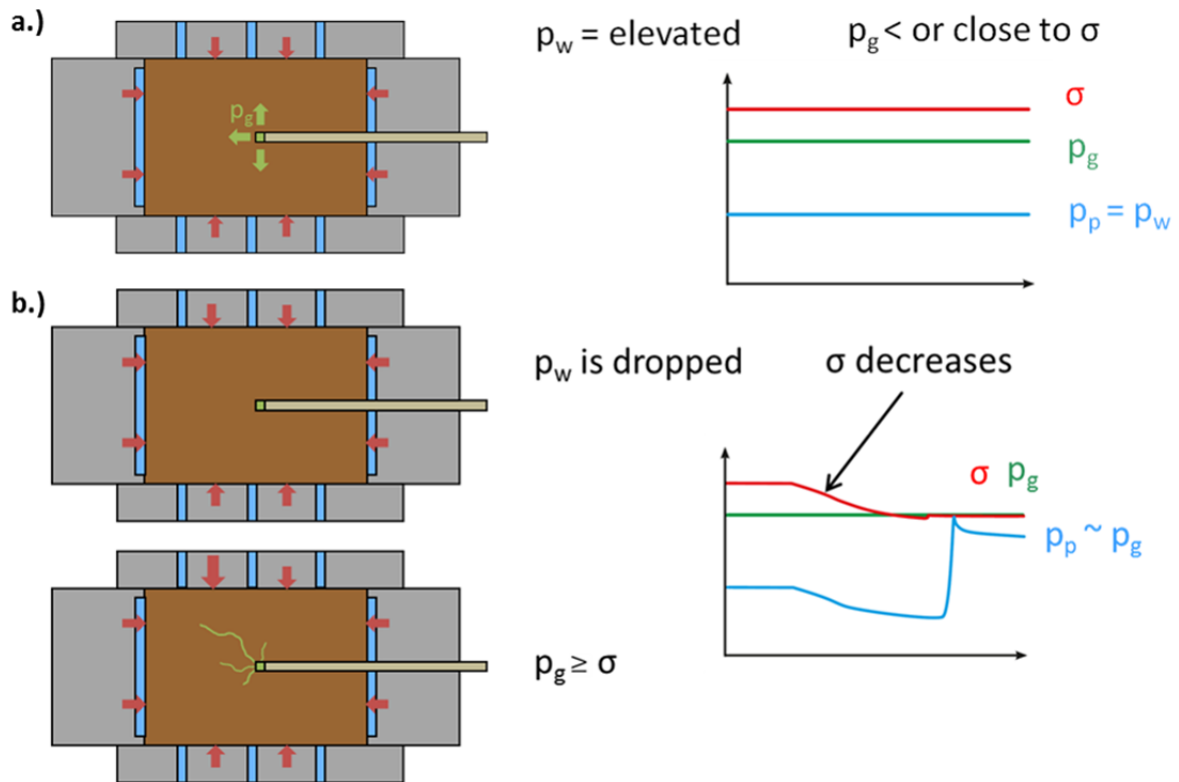


954

955 **Figure 5** - Sample Mx80-14. a.) The initial gas breakthrough event. A transient outflow occurred  
 956 apparently spontaneously (day 413.8). The clay quickly began to self-seal and outflow ceased. A  
 957 phase of pressure cycling followed, with associated transient outflows and subsequent self-sealing.  
 958 Gas migration during this phase was highly episodic, displaying extreme cyclicality and temporal. b.)  
 959 Variation in local stresses during pressure cycling.

960

961



962

963 **Figure 6** – Schematic representation of gas entry under a constant applied  $p_g$  condition and at  
 964 elevated  $p_w$  conditions. a.) Initial state with gas pressure held constant, at or below the total stress.  
 965 b.) Gas entry instigated by dropping  $p_w$  and allowing stresses to decline. Entry only occurs once  
 966 local total stress falls below the applied gas pressure. Pressure cycling and episodic behaviour may  
 967 occur during this phase as the clay is ‘worked’ to form stable pathways. No evidence was found for  
 968 elevated pore-water conditions impacting on the gas entry behaviour of the bentonite.

969

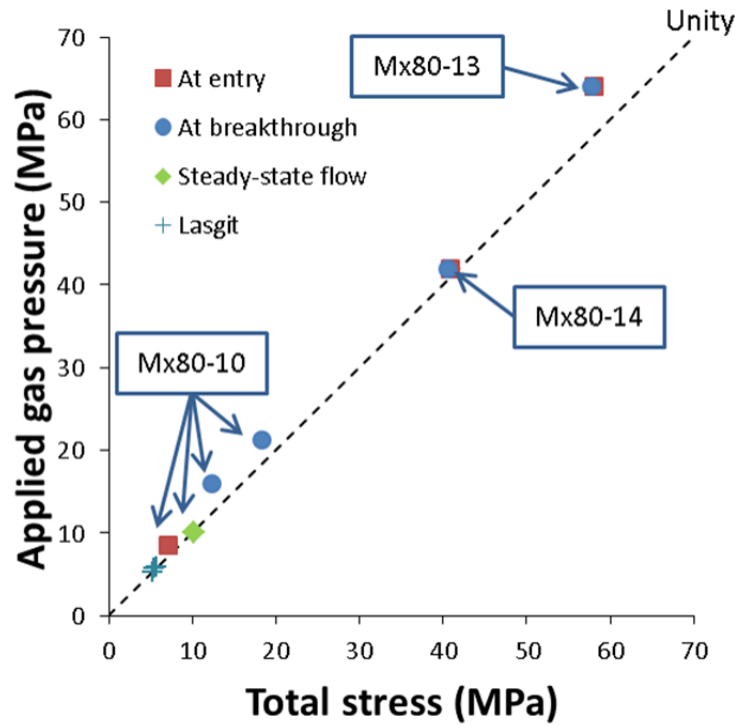
970

971

972

973

974



975

976 **Figure 7** – Cross-plot showing key parameters for several gas injection tests. The general coupling  
 977 between gas pressure and total stress is clearly evident. Once steady-state flow is achieved,  $p_g$  falls  
 978 closer to  $\sigma$ . The dotted line represents unity.